Zeitschrift: IABSE publications = Mémoires AIPC = IVBH Abhandlungen

Band: 36 (1976)

Artikel: Failure mechanisms for reinforced concrete beams in torsion and bending

Autor: Müller, P.

DOI: https://doi.org/10.5169/seals-929

Failure Mechanisms for Reinforced Concrete Beams in Torsion and Bending

Mécanismes de ruine pour des poutres en béton armé soumises à la torsion et à la flexion

Bruchmechanismen für Stahlbetonbalken unter Torsion und Biegung

P. MÜLLER
Research Associate, Institute of Structural Engineering, Swiss Federal Institute of Technology (ETH), Zurich (Switzerland).

Introduction

To describe the failure of reinforced concrete beams with thin-walled closed cross section in torsion and bending, LAMPERT [2, 3] used a space truss model based on the lower bound theorem of the Theory of Plasticity. The good correspondence between theory and test results stimulates to generalize the model. The application of the Theory of Plasticity to the general plane stress problem of reinforced concrete shear walls [5] has led to a better understanding of the collapse mechanisms of these beams. Indeed all collapse mechanisms, known so far, turn out to be incompatible with the state of stress assumed in the truss model.

The aim of this contribution is to develop new compatible mechanisms. The very simple basic mechanism has significance for engineering practice in allowing easy visualization of the failure modes assumed by the truss model. The truss model and the new mechanisms supply together, as lower and upper bound solutions, respectively, the exact interaction relation for thin-walled closed cross sections subjected to torsion and bending.

We confine ourselves to constant bending moment and torque, and, for simplicity, to rectangular cross sections. The present work is part of the study [5] which the reader is referred to for general cross sections and detailed information.

Basic Theory

The present investigation is based on the classical Theory of Plasticity, e.g. [1], in particular on the concept of plastic potential and on the upper and lower bound theorems of limit analysis. The latter is based on the following idealizations and assumptions:

1. A rigid-perfectly plastic or elastic-perfectly plastic material is visualized (Fig. 1).

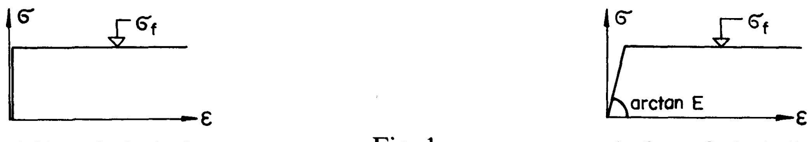

Fig. 1.

2. The elastic and plastic deformations are small in the sense of no significant changes in the geometry of the structure, so as to allow the formulation of equilibrium equations for the original configuration.

Yield Criterion for Reinforced Concrete Shear Walls

The following assumptions are postulated:

1. The assumptions of the Theory of Plasticity in the sense of Section 2 are admissible.
2. The concrete is assumed to be in a state of plane compressive stress; in particular, the tensile strength of concrete is neglected.
3. The reinforcement is idealized as a state of plane stress in its direction.
4. The assumed redistribution of steel and concrete stresses stipulates for full aggregate interlock and dowel action in initial cracks. Local and bond failure are excluded.
5. The range of ratio of reinforcement is such that:
   a) no failure occurs at first crack formation;
   b) compressive strength of concrete is never reached.
6. The reinforcement is placed as a orthogonal net.

Assumption 1, in particular, the necessary ductility of failure, is sufficiently confirmed by [6, 7, 8]. 5b) and 6) are not postulated in [5]. But as the yield criterion merely serves to develop mechanisms compatible with the space truss model, we do not need more generality.

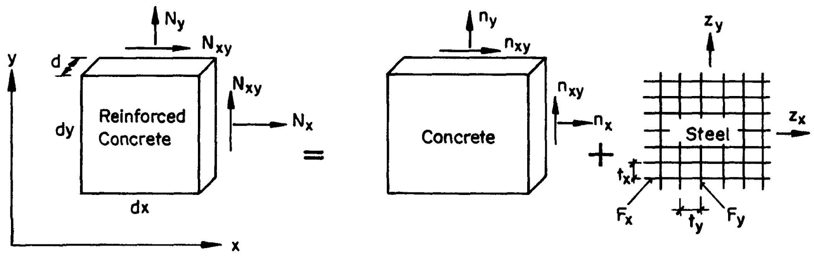

Fig. 2.

The membrane forces N_x, N_y, N_{xy}, acting on the differential element of Figure 2, are equivalent to the sum of the stress resultants n_x, n_y, n_{xy} of the concrete and z_x, z_y of the reinforcement. It is convenient to introduce the coordinate system (x, y) parallel to the orthogonal reinforcement.

$$\left.\begin{aligned} N_x &= n_x + z_x \\ N_y &= n_y + z_y \\ N_{xy} &= n_{xy} \end{aligned}\right\} \tag{1}$$

$$\text{where } z_x = \frac{\sigma_e F_x}{t_x},\ z_y = \frac{\sigma_e F_y}{t_y}. \tag{2}$$

The concrete stress not reaching compressive strength, the only yield condition is

$$n_I = \frac{n_x + n_y}{2} + \sqrt{\left(\frac{n_x - n_y}{2}\right)^2 + n_{xy}^2} \leq 0,$$

$$\text{or } n_{xy}^2 \leq n_x\, n_y, \quad n_x \leq 0, \quad n_y \leq 0, \tag{3}$$

whereas steel is governed by the yield criterion

$$\left.\begin{aligned} |z_x| &\leq P_x = \frac{\sigma_f F_x}{t_x}, \\ |z_y| &\leq P_y = \frac{\sigma_f F_y}{t_y}, \end{aligned}\right\} \tag{4}$$

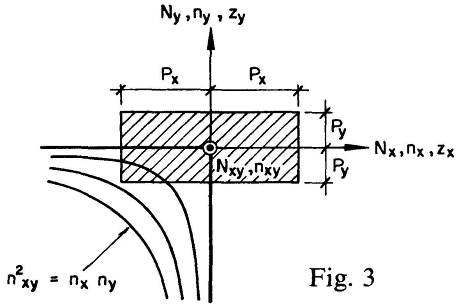

Fig. 3

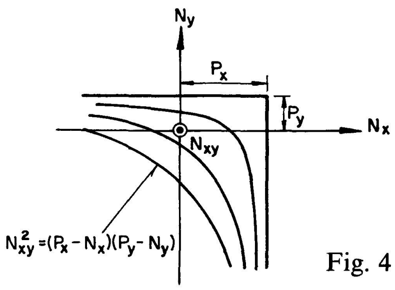

Fig. 4

In the three-dimensional space of stresses (Fig. 3) the yield surface of the concrete is an elliptic cone, while the yield locus of the reinforcement is represented by a rectangle in the plane (N_x, N_y). The sets of stress points with the properties (3) and (4) are convex sets. Hence, the convex set of stress points, satisfying the unknown yield criterion $\Phi(N_x, N_y, N_{xy}) \leq 0$, is defined by (1) as a linear combination of the convex sets defined by (3) and (4); i.e. Φ is found to be the envelope of all translationally shifted yield loci of concrete with centre within the shaded rectangle of Figure 3. Hence, Φ is represented by the concrete cone with tip at the point (P_x, P_y, 0) as illustrated in Figure 4, and the yield criterion may be written

$$\left.\begin{aligned} &\Phi_1 = N_{xy}{}^2 - (N_x - P_x)(N_y - P_y) \leq 0, \\ &\Phi_2 = N_x - P_x \leq 0, \Phi_3 = N_y - P_y \leq 0. \end{aligned}\right\} \tag{5}$$

Considering assumption 5b), the yield criterion (5) coincides with that reported by NIELSEN [10].

For stress points (N_x, N_y, N_{xy}) on the yield surface (5), the stress resultants in the components steel and concrete are

$$\left.\begin{aligned} &z_x = P_x,\ z_y = P_y, \\ &n_{xy}^2 = n_x n_y, \quad n_x \leq 0, \quad n_y \leq 0, \\ \text{or} \quad &n_{II} \leq n_I = 0, \end{aligned}\right\} \tag{6}$$

where n_I and n_{II} denote the major and minor principle concrete stress, respectively. Thus both components of reinforcement are yielding, while the concrete is in a uniaxial state of compressive stress. Evidently this coincides completely with the state of stress, the truss model is based on.

The longitudinal reinforcement and the stirrups of the shear wall shown in Figure 5 are interpreted as stringers and posts of a truss, whose struts idealize a uniform state of compressive stress in the concrete. The inclination of the struts is determined from the condition that both the longitudinal and the stirrup reinforcement are yielding. Assumption 5b is taken for granted.

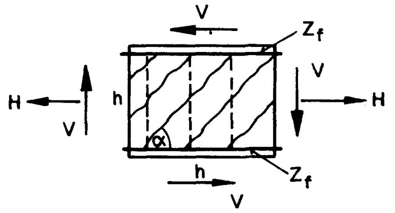

Fig. 5.

Whereas the truss model and the foregoing more general results harmonize with respect to the statical aspects, care is needed however in the translation of the kinematics of a truss to reinforced concrete shear walls.

Yield Law and Kinematics

For states of stress at the yield limit (5), with non-zero N_{xy}, the following is true

$$\Phi_1 = 0, \Phi_2 < 0, \Phi_3 < 0, \tag{7}$$

and hence, according to the theory of plastic potential, the rates of plastic strain are related to the stresses as follows

$$\left.\begin{aligned} \dot{\varepsilon}_x &= \dot{\lambda}\frac{\partial \Phi_1}{\partial N_x} = -\dot{\lambda}(N_y - P_y) = -\dot{\lambda} n_y, \\ \dot{\varepsilon}_y &= \dot{\lambda}\frac{\partial \Phi_1}{\partial N_y} = -\dot{\lambda}(N_x - P_x) = -\dot{\lambda} n_x, \\ \dot{\gamma}_{xy} &= \dot{\lambda}\frac{\partial \Phi_1}{\partial N_{xy}} = \dot{\lambda}(2N_{xy}) = \dot{\lambda} 2 n_{xy}, \\ &\text{where } \dot{\lambda} \geq 0. \end{aligned}\right\} \tag{8}$$

Substituting the expressions (8) into (7) we find that

$$\left(\frac{\dot{\gamma}_{xy}}{2}\right)^2 = \dot{\varepsilon}_x \dot{\varepsilon}_y, \qquad \dot{\varepsilon}_x \geq 0, \dot{\varepsilon}_y \geq 0, \tag{9}$$

or, $\dot{\varepsilon}_I$ and $\dot{\varepsilon}_{II}$ denoting the major and minor principle strain-rate, respectively,

$$\dot{\varepsilon}_I \geq \dot{\varepsilon}_{II} = 0. \tag{10}$$

If $\Phi_1 = \Phi_2 = \Phi_3 = 0$, (10) is replaced by (11).

$$\dot{\varepsilon}_I \geq \dot{\varepsilon}_{II} \geq 0. \tag{11}$$

Thus the only velocity fields compatible with the considered stress fields are those with no compressive strains. (10) and (11) are merely the dual kinematical interpretation of assumption 5b preventing concrete crushing. Although this consequence of the upper limitation of reinforcement ratios seems somewhat trivial, it has been overlooked in all torsional collapse mechanisms proposed so far. Above all this is due to the fact that the yield criterion (5) and assumption 5b have only been used implicitly.

Calculating the direction of the minor principal strain-rate $\dot{\varepsilon}_{II} = 0$ in (10), there results

$$\tan 2\alpha = \frac{-\dot{\gamma}_{xy}}{\dot{\varepsilon}_y - \dot{\varepsilon}_x} = \frac{-2N_{xy}}{-(N_x - P_x) + (N_y - P_y)} = \frac{-2n_{xy}}{n_y - n_x} \tag{12}$$

Now the last expression in (12) equals the direction of concrete compressive trajectories. Thus the principal axis of plastic strain-rates and those of concrete stress-state coincide. Considering (9) in (12) we obtain

$$\tan 2\alpha = \frac{-\dot{\gamma}_{xy}}{\dot{\varepsilon}_y - \dfrac{\dot{\gamma}_{xy}^2}{4\dot{\varepsilon}_y}} = \frac{2\left(\dfrac{-\dot{\gamma}_{xy}}{2\dot{\varepsilon}_y}\right)}{1 - \left(\dfrac{-\dot{\gamma}_{xy}}{2\dot{\varepsilon}_y}\right)^2} = \frac{2\tan\alpha}{1 - (\tan\alpha)^2} \tag{13}$$

By means of tan α, (9) may also be expressed parametrically by two equations from (14) and (15)

$$\tan\alpha = \frac{-\dot{\gamma}_{xy}}{2\dot{\varepsilon}_y} = \frac{2\dot{\varepsilon}_x}{-\dot{\gamma}_{xy}} = \pm\sqrt{\frac{\dot{\varepsilon}_x}{\dot{\varepsilon}_y}}, \tag{14}$$

$$-\dot{\gamma}_{xy} = \frac{\dot{\varepsilon}_x}{\tan\alpha} + \dot{\varepsilon}_y \tan\alpha, \tag{15}$$

where $\dot{\varepsilon}_x \geq 0$, $\dot{\varepsilon}_y \geq 0$.

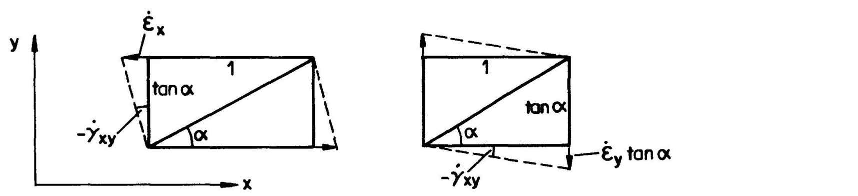

Fig. 6.

On the other hand, if we derive the kinematic relations using a truss with rigid strut, as shown in Figure 6 [2, 3], we only obtain equation (15). The kinematics of a truss does not correspond with the kinematics of shear walls governed by the flow rules (8). The truss only prevents compressive strains in the direction of the struts and therefore neglects the solid nature of the shear wall.

Discontinuities in the Velocity Field

From the Theory of Plasticity we know that the velocity fields associated with collapse often are discontinuous. Therefore, we further have to derive the restrictions imposed to velocity jumps by (10). In doing so we have to visualize a discontinuity line as the limiting case of a finite transition layer with rapidly but continuously (e.g. linearly) changing velocities as shown in Figure 7.

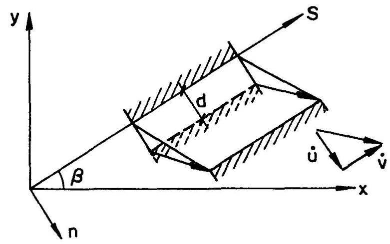

Fig. 7.

The depth of the transition layer tending toward zero, the plastic strain-rates are

$$\left.\begin{aligned} &\dot{\varepsilon}_n = \frac{\dot{u}}{d}, \quad \dot{\varepsilon}_t = 0, \quad \dot{\gamma}_{nt} = \frac{\dot{v}}{d}, \\ &\dot{\varepsilon}_I = \frac{1}{2}\left(\frac{\dot{u}}{d} + \sqrt{\left(\frac{\dot{u}}{d}\right)^2 + \left(\frac{\dot{v}}{d}\right)^2}\right), \ \dot{\varepsilon}_{II} = \frac{1}{2}\left(\frac{\dot{u}}{d} - \sqrt{\left(\frac{\dot{u}}{d}\right)^2 + \left(\frac{\dot{v}}{d}\right)^2}\right) \end{aligned}\right\} \quad (16)$$

Evidently (10) is only true, provided that

$$\dot{u} \geq 0, \dot{v} = 0. \quad (17)$$

Thus only the normal velocity component may jump, and discontinuity lines and concrete compressive trajectories coincide in direction, viz. $\alpha = \beta$. Now the physical crack pattern observed in tests tends towards the theoretical pattern of concrete compressive trajectories at collapse state [6-9]. We therefore may regard discontinuities governed by (17) as the cracks of the ideal rigid-plastic shear wall obeying (8), and we name them *collapse cracks.* (17) has been adopted in [4] in the following concise form: collapse cracks open normally to their direction. It must be emphasized that, for an elastic-perfectly plastic material, the statement only refers to the increments of crack widening at collapse state.

On the other hand, if there is also a jump in the tangential velocity component, viz. $\dot{v} \neq 0$, we obtain from (16) $\dot{\varepsilon}_I \geq 0$, $\dot{\varepsilon}_{II} \leq 0$. Hence, the concrete is crushing, and its contribution to the rate of energy dissipation must not be neglected. $\dot{\gamma}_{nt}$ being non-zero, the discontinuity lines and the concrete compressive trajectories coincide no more. Because the physical crack pattern, prior to failure, again tends toward concrete compressive trajectories, rather than toward the possible discontinuity lines, we avoid the term "crack" for the latter. According to the Theory of Plasticity for plane stress and strain such discontinuities are named *slip lines.* Thus "collapse crack" is reserved in its original meaning for discontinuities with no concrete crushing, whereas "slip lines" always imply concrete crushing. Together with a yield criterion including concrete crushing, such slip lines are studied in reference [5] in the context of shear in reinforced concrete and shear walls in general. In this connection, the reader is also referred to reference [11] recently published, where partially similar results have been derived independently.

The results of this Section may be summarized as follows: Only collapse cracks but not slip lines are compatible with the yield criterion (5).

Reinforced Concrete Beams in Torsion and Bending

To prepare the derivation of a new mechanism, the space truss model [2, 3] and two mechanisms incompatible with the latter [2, 12] are recapitulated, as lower and upper bound approaches respectively to the ultimate strength of reinforced concrete beams in torsion and bending. From the theoretical point of view, it must be pointed out that the space truss model intrinsically applies to thin-walled closed cross sections. Hence, mechanisms compatible with the latter must be derived for the same statical system. The applicability of the same relations to solid cross sections is well confirmed by test results [6, 7, 8], but is not followed up theoretically in this study.

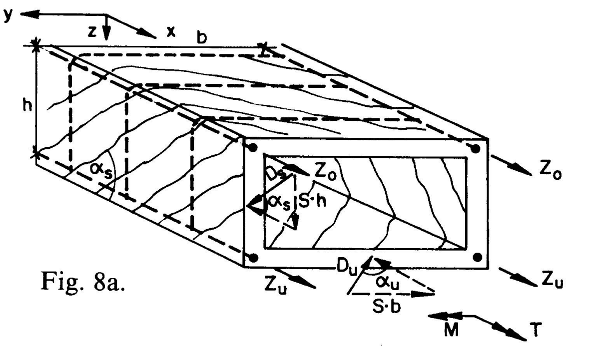

Fig. 8a.

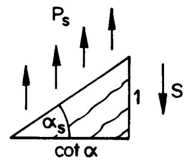

Fig. 8b.

Consider a beam with thin-walled closed rectangular cross section as shown in Figure 8a, for example. The longitudinal reinforcement is concentrated in four corner stringers of equal yield force Z_f. The yield forces of the stirrups, measured per unit length, equal P_u in the top and bottom shear walls and P_s in the side shear walls. The reinforcement ratio is within the range of no concrete crushing.

In the space truss model the concrete is assumed to be in a uniaxial state of compressive stress being uniform in each shear wall. Hence, the inclination of struts α and the shear flow S are uniform in each wall, the resultant of concrete stresses is acting in the centre of the wall, and the bending moment is sustained only by the top and bottom walls. The bending moment and the torque being constant, it is further assumed that the stringer forces are constant along the beam, or equivalently, that the shear flow S is constant around the sectional perimeter. For convex cross sections the reinforcement of all but one shear wall must reach the yield stress. Thus, for positive bending moment, only the reinforcement forces of the top wall are unknown. Conveniently the equilibrium equations of moments are then formulated relative to the x- and y-axis lying in the top wall

$$M = 2Z_f h - 2Sh \cot \alpha_s \tfrac{h}{2} - Sb \cot \alpha_u h, \tag{18}$$

$$T = 2Sh \tfrac{b}{2} + Sbh = 2S \cdot bh = 2SF_0. \tag{19}$$

From the free-body diagram Figure 8b we obtain

$$S = P_s \cot \alpha_s = P_u \cot \alpha_u. \tag{20}$$

In particular, (20) implies also that the strut inclinations of the side walls are the same, what we already have used in (18). Substituting from (19) and (20) into (18) we obtain the interaction relation

$$M = 2Z_f h - \frac{T^2}{4F_0}\left(\frac{h}{b}\frac{1}{P_s} + \frac{1}{P_u}\right) \tag{21}$$

The same relation may also be derived directly by means of the yield criterion (5), each shear wall being in a uniform state of membrane stress N_x, N_y, N_{xy}. To be a lower bound solution, the loads must be applied by rigid diaphragms. Additionally, proper anchorage of longitudinal reinforcement has to be ensured by an anchorage region, for which statically admissible stress fields must be found satisfying the end boundary conditions. However, within the beam theory these problems may be regarded as constructive problems. The transition from the space structure to the beam is effected by the transition from the yield criterion (5) to the yield criterion (21) in the generalized stresses acting on the differential beam element. Static boundary conditions are satisfied then in the generalized stresses. In this sense the truss model solution is a lower bound to the exact interaction relation. To have a complete solution, we still must find a mechanism related to the assumed state of stress by (8).

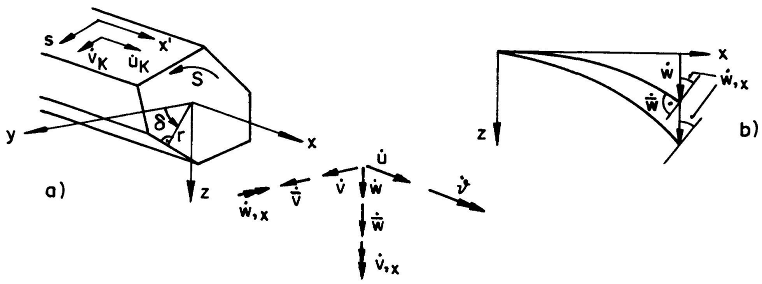

Fig. 9.

In [2] the usual assumption of beam theory is postulated: Cross sections normal to the beam axis remain plane. The velocities $\dot{u}_K$, $\dot{v}_K$ of shear wall K are related (Fig. 9) to the displacement parameter rates $\dot{u}$, $\dot{v}$, $\dot{w}$, $\dot{\bar{v}}$, $\dot{\bar{w}}$, $\dot{\vartheta}$ of the beam axis by

$$\left.\begin{aligned} \dot{u}_K &= \dot{u} - z\dot{w}_{,x} - y\,\dot{v}_{,x}, \\ \dot{v}_K &= -(\dot{v} + \dot{\bar{v}})\sin\delta + (\dot{w} + \dot{\bar{w}})\cos\delta + r\dot{\vartheta}, \end{aligned}\right\} \tag{22}$$

where v, w and $\bar{v}$, $\bar{w}$ result from pure bending and pure shearing, respectively, as shown in Figure 9b. $(\ )_{,x}$ and $(\ )_{,s}$ denote differentiation with respect to the x- and s-direction. The rates of strain are

$$\left.\begin{aligned} \dot{\varepsilon}_{LK} &= \dot{u}_{K,x} = \dot{u}_{,x} - z\dot{w}_{,xx} - y\dot{v}_{,xx}, \\ \dot{\gamma}_K &= \dot{u}_{K,s} + \dot{v}_{K,x} = -\dot{\bar{v}}_{,x}\sin\delta + \dot{\bar{w}}_{,x}\cos\delta + r\dot{\vartheta}_{,x}. \end{aligned}\right\} \tag{23}$$

Hence, the rate of longitudinal extension $\dot{\varepsilon}_{LK}$ varies linearly across the wall, whereas the shear strain-rate $\dot{\gamma}_K$ is constant (Fig. 10).

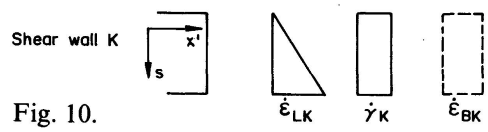

Fig. 10.

Considering (14): $\quad \tan \alpha_K = \dfrac{2\dot{\varepsilon}_{LK}}{\dot{\gamma}_K},$

the strut inclination varies linearly in each wall too. Hence, the mechanism is not compatible with the constant stress-state of the space truss model. Assuming in each wall a constant distribution of the stirrup strain-rate $\dot{\varepsilon}_{BK}$, and calculating $\dot{\varepsilon}_{BK}$ with (9) for the average rate of longitudinal extension $\dot{\varepsilon}_{LK}$ in the centre of the wall, we may derive (21). However, (9) is violated in general. If the contribution of concrete crushing to the rate of energy dissipation, in regions with $\dot{\gamma}_K{}^2 > 4\dot{\varepsilon}_{LK} \cdot \dot{\varepsilon}_{BK}$, would not be neglected, ultimate strength would be higher than (21).

An upper bound approach with discontinuous velocity fields is the well known "Skew Bending" mechanism [12].

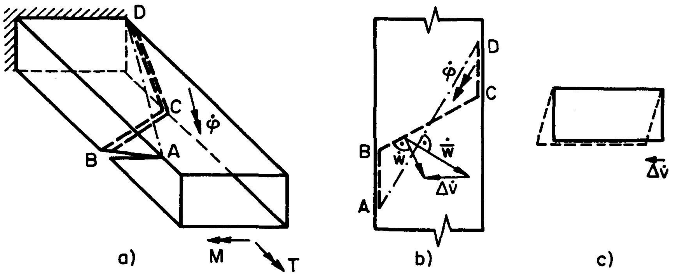

Fig. 11a, b, c.

Consider a rotation of the free end of the cantilever with thin-walled cross section shown in Figure 11a, about a skew axis AD. The position of the axis is fixed by the two ends of a crack ABCD running around the beam. The fact that the load factors derived from this mechanism are lower than predicted by (21), has erroneously been explained by nodal forces [13]. The true reason may be easily recognized from the top view Figure 11b. If the sectional shape is preserved as usually assumed, there must be a jump in the tangential velocity component along the discontinuity line BC in the bottom wall. Hence, the contribution of concrete crushing to the rate of energy dissipation must not be neglected, and higher load factors than predicted by (21) would be obtained, if concrete strength is assumed according to assumption 5b.

On the other hand, if only the normal velocity component is assumed to jump along ABCD, a sectional deformation $\Delta\dot{v}$ is forced upon the free end of the cantilever (Fig. 11b, c).

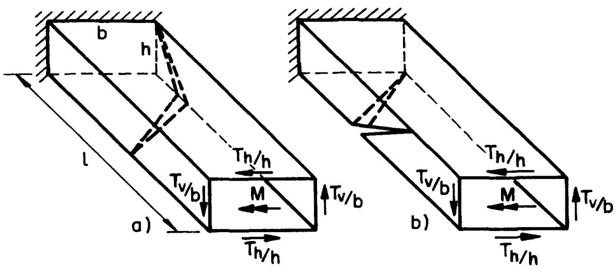

Fig. 12.

However, for a cantilever regarded as a folded structure, lower load factors may be obtained with mechanisms as suggested in Fig. 12. Because of the deformable cross section the results depend on the ratio of T_v and T_h, i.e. of the torques applied to the vertical and horizontal walls, respectively. For cantilevers of sufficient length, the load factors are always lower than predicted by (21). The latter is reached only for $T_v = T_h = T/2$, i.e. for the optimal load application corresponding to constant shear flow.

On the other hand, combining appropriately the two mechanisms shown in Figure 12a and Figure 12b, we may assume a non-deformable cross section without violating (17). This mechanism is treated in detail in the next Section. The resulting interaction relation coincides with (21), and the strut inclinations correspond to constant shear flow. Hence, the statical assumption of constant shear flow corresponds evidently to the kinematical assumption of a non-deformable cross section. This corresponds also to the assumption of a rigid diaphragm in (21), which prevents the mechanisms of Figure 12.

Discontinuous Failure Mechanism

First a compatible mechanism with discontinuous velocity fields is derived. It allows not only easy visualization, but is also the basic element of all other continuous and discontinuous compatible mechanisms. As in the statical approach we only allow for membrane forces, and all resistance of the shear walls normal to their plane is neglected.

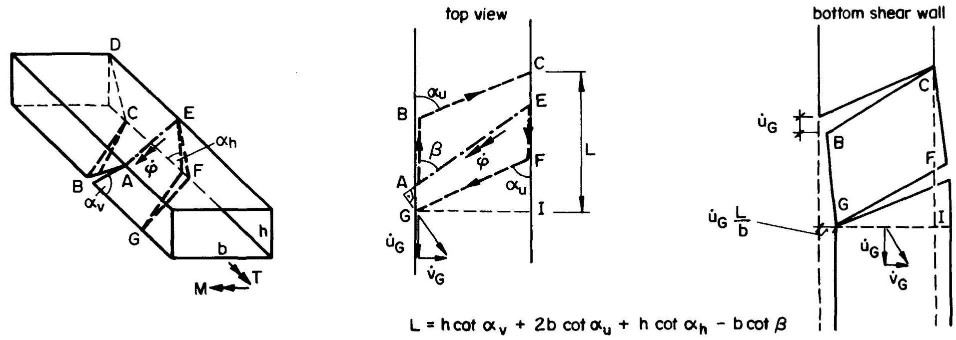

Fig. 13.

Consider again a rigid rotation of the front part of the beam shown in Figure 13 about a skew axis AE situated for instance in the top wall. However, contrary to Figure 11, the inclination β of the axis of rotation is not determined from the position of the ends of *one* crack, but is an additional parameter to be determined from condition (17) and from the assumption that the sectional shape is preserved.

Consequently, *two* cracks have to be considered, starting from the points A and E of the axis of rotation. The hinge AE opens in the front wall the collapse crack AB, which, on his part, opens the crack BC in the bottom wall. At C the crack must be closed again, because there is no hinge in the top wall at D.

The same is true for the collapse crack EFG. The two cracks running around the beam separate in the bottom wall the portion BCFG being connected along the sides CF and BG with the fixed and the rotating part of the beam, respectively. Considering (17), the portion BCFG undergoes a rigid rotation in its plane.

Now, if the shape of cross section GI is preserved, the velocities of point G, in the plane of the bottom shear wall, are (top view)

$$\left.\begin{aligned} \dot{u}_G &= \dot{\varphi} h \sin\beta, \\ \dot{v}_G &= \dot{\varphi} h \cos\beta. \end{aligned}\right\} \tag{24}$$

On the other hand, considering the rigid body rotation of the portion BCFG in the bottom wall (Fig. 13 bottom shear wall), we obtain

$$\dot{v}_G = \dot{u}_G \tfrac{L}{b}, \tag{25}$$

where, according to Figure 13, L is a function of the inclination β of the axis of rotation and of the free parameters of the mechanism, that is the inclinations α of the collapse cracks. Considering (24) in (25) and substituting for L we find

$$\cot\beta = \tfrac{L}{b} = \tfrac{1}{2}(\cot\alpha_v + \cot\alpha_h)\tfrac{h}{b} + \cot\alpha_u. \tag{26}$$

The mechanism satisfies condition (17) everywhere, and a deformation of the cross section is prevented for arbitrary crack inclinations by choosing the ratio of twist and flexural curvature $\cot\beta$ according to (26). In particular, referring again to the example of Figure 8a, we may use the crack inclinations (20) obtained by the space truss model. Hence, the mechanism is compatible with the state of stress assumed in the lower bound approach, and the interaction relation (21) corresponds to the limit load of a beam with non-deformable cross section, within the scope of membrane theory.

To verify the statement, we equate the rate of external work

$$L_a = \dot{\varphi}\sin\beta\, M + \dot{\varphi}\cos\beta\, T \tag{27}$$

to the rate of energy dissipation

$$L_d = \dot{\varphi}\sin\beta\,\{h^2 \tfrac{1}{2}(\cot^2\alpha_v + \cot^2\alpha_h) P_s + hb\cot^2\alpha_u P_u + 2Z_f h\}, \tag{28}$$

and considering (26) we obtain

$$\left.\begin{aligned} M = 2Z_f h &+ \tfrac{1}{2}(h^2 P_s \cot^2\alpha_v - \tfrac{h}{b} T\cot\alpha_v) \\ &+ \tfrac{1}{2}(h^2 P_s \cot^2\alpha_h - \tfrac{h}{b} T\cot\alpha_h) \\ &+ \tfrac{b}{h}(h^2 P_u \cot^2\alpha_u - \tfrac{h}{b} T\cot\alpha_u). \end{aligned}\right\} \tag{29}$$

Minimizing M for fixed T with respect to the crack inclinations we find

$$2\frac{\partial M}{\partial(\cot\alpha_v)} = 2h^2 P_s \cot\alpha_v - \tfrac{h}{b}T = 0,$$

and

$$\cot\alpha_v = \frac{T}{2bh}\frac{1}{P_s} = \frac{T}{2F_0}\frac{1}{P_s}.$$

Hence,

$$\cot\alpha_v = \cot\alpha_h = \frac{S}{P_s}, \quad \cot\alpha_u = \frac{S}{P_u}, \tag{30}$$

and by substitution into (29) relation (21) is obtained again:

$$M = 2Z_f h - \frac{T^2}{4F_0}\left(\frac{h}{b}\frac{1}{P_s} + \frac{1}{P_u}\right). \tag{21}$$

To get the whole range of interaction, we also have to consider the mechanisms with axis of rotation in the other shear walls. For pure torsion all the reinforcement is yielding in our example. Hence, each of these mechanisms is possible. In particular, a mechanism with pure twist and extension, as shown in Figure 14, is also feasible. It may be regarded as a linear combination of the two mechanisms with axis of rotation in the top and bottom shear wall.

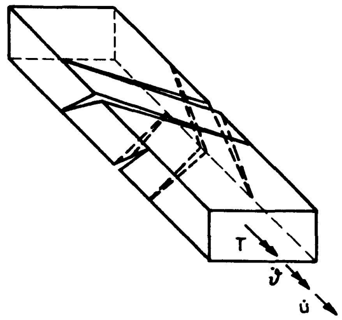

Fig. 14.

Finally, there should be pointed out that the length of the presented discontinuous mechanism, i.e. in our example

$$l_{Min} = h \cot \alpha_v + b \cot \alpha_u, \tag{31}$$

evidently is the minimum failure region required by a mechanism satisfying the conditions of no concrete crushing and no cross-sectional deformations. If the most critical part of the beam is shorter than the minimal failure length calculated with the corresponding reinforcement, (21) is to be regarded as a lower bound.

Continuous Mechanisms and Beam Theory

Spreading the rotation $\dot{\varphi}$ in the top wall and the cracks over a finite length d we get a continuous mechanism as shown in Figure 15a. All relations still hold, if the reinforcement does not change over the additional length. Evidently it is not possible in general to describe these mechanisms by beam theory, which relates the displacements within a cross section to displacement parameters of the beam axis. Only in the case illustrated in Figure 15b this is partially possible.

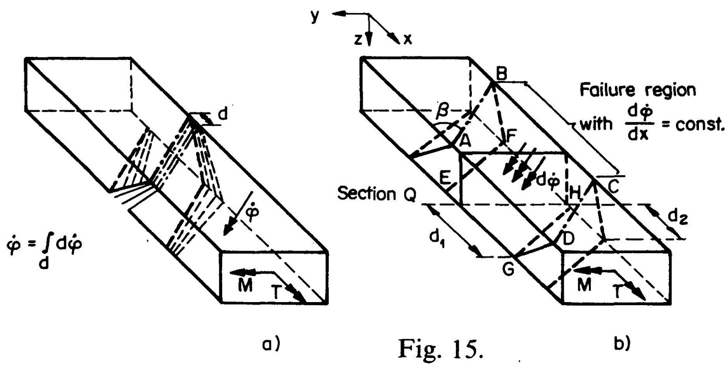

Fig. 15.

Consider a continuous mechanism with constant curvature-rate of the top wall within the zone ABCD, viz. $d\dot{\varphi}/dx = \text{const.}$, and hence, with a zone of uniform strain-rates EFGH in the bottom wall. If the failure region is long enough, as shown in Figure 15b, there exist sections Q lying completely within the region ABEF-CDGH. Obviously cross sections Q have plane strain-rate distributions, and all their longitudinal fibers have the same curvature. Thus beam theory may be used for these sections. On the other hand, looking at the different distances d_1, d_2 between the section corners and the rigid parts of the beam, and considering that the rate of extension is the same for d_1 and d_2 and is zero in the top wall, we find that originally plane sections do not remain plane.

Hence, the beam assumptions (22) must be completed by warping terms. Referring again to Figure 9, the in-plane velocities of shear wall K are

$$\left.\begin{aligned} \dot{u}_K &= \dot{u} - z\,\dot{w}_{,x} - y\,\dot{v}_{,x} + \dot{U}(s), \\ \dot{v}_K &= -\dot{v}\sin\delta + \dot{w}\cos\delta + r\dot{\vartheta} + \dot{V}(s), \end{aligned}\right\} \tag{32}$$

where the terms $\dot{U}$, $\dot{V}$, $r\dot{\vartheta}$ account for warping, stirrup elongation and the assumption of a non-deformable cross section, respectively. The strain-rates $\dot{\varepsilon}_{LK}$, $\dot{\varepsilon}_{BK}$ of the longitudinal and stirrup reinforcement, respectively, and the shear strain-rates $\dot{\gamma}_K$ are

$$\left.\begin{aligned} \dot{\varepsilon}_{LK} &= \dot{u}_{K,x} &&= \dot{u}_{,x} - z\dot{w}_{,xx} - y\dot{v}_{,xx}, \\ \dot{\varepsilon}_{BK} &= \dot{v}_{K,s} &&= \dot{V}_{,s} \\ \dot{\gamma}_K &= \dot{u}_{K,s} + \dot{v}_{K,x} &&= \dot{U}_{,s} + r\dot{\vartheta}_{,x}. \end{aligned}\right\} \tag{33}$$

Contrary to equation (23) the shear strain-rate distribution across a wall depends now additionally on a warping term to be determined appropriately. Assuming a constant $\tan\alpha_K$ in each shear wall according to the state of stress in the truss model and considering (14) we find a linear variation of all strain-rate components:

$$\left.\begin{aligned} &\dot{\gamma}_K = 2\dot{\varepsilon}_{LK}\cdot\cot\alpha_K, \quad \dot{\varepsilon}_{BK} = \dot{\varepsilon}_{LK}\cot{}^2\alpha_K, \\ &\dot{\varepsilon}_{LK} \geq 0, \quad \dot{\varepsilon}_{BK} \geq 0. \end{aligned}\right\} \tag{34}$$

Integrating (33) and substituting from (34) we obtain

$$\left.\begin{aligned} \dot{U}(s) &= \int_s (2\dot{\varepsilon}_{LK}\cot\alpha_K - r\dot{\vartheta}_{,x})\,ds, \\ \dot{V}(s) &= \int_s \dot{\varepsilon}_{LK}\cot{}^2\alpha_K\,ds. \end{aligned}\right\} \tag{35}$$

Continuity of the $\dot{u}_K$ around the closed cross section is ensured, provided that

$$\oint_s \dot{U}_{,s}\,ds = 0 = \oint_s \dot{\gamma}_K\,ds - \dot{\vartheta}_{,x}\oint_s r\,ds,$$

$$\text{hence } \dot{\vartheta}_{,x} = \frac{1}{2F_0}\oint_s 2\dot{\varepsilon}_{LK}\cot\alpha_K\,ds. \tag{36}$$

$\tan\alpha_K$ being substituted from equation (20), the strain-rates are everywhere compatible with the state of stress assumed in the truss model. For zero strain-rates in the top wall of our example, equation (36), together with (33), evidently gives the same ratio of twist and curvature as equation (26).

However, it must be emphasized that the pure sectional or beam analysis, i.e. equations (32)-(36) alone, do not yet represent a kinematically admissible mechanism. Since the plastified sections are warping, kinematic boundary conditions are violated at cross sections separating rigid and plastified parts of the beam. In other words: Equations (35), (36), (33) imply that the parameters $\dot{u}_{,x}$, $\dot{\vartheta}_x$, $\dot{w}_{,xx}$, $\dot{v}_{,xx}$ are constant along the beam axis. This corresponds to the primary assumption that cross sections Q lay completely within the region ABEF-CDGH. To be kinematically admissible, the beam mechanism must be completed at the ends with the more general mechanisms of Figure 15a and consequently corresponds to the mechanism shown in Figure 15b.

Assuming no change in the reinforcement within the failure region, and equating the rate of external work to the rate of energy dissipation for the mechanism of Figure 15b as well as for the differential beam element governed by (32)-(36), we obtain the interaction relation (21). Hence, although a pure sectional mechanism does not exist, the modified sectional approach is valid, standing for a mechanism of the type of Figure 15b. In particular, the essential results concerning arbitrary cross sections in [2] are preserved.

Finally, we realize that the presence of shear forces in general is inconsistent with the assumption of a plane strain-rate distribution over a cross section according to (32)-(36).

As shown in Figure 15b, this assumption implies that the longitudinal reinforcement is yielding over a long failure region. For step-wise constant longitudinal reinforcement, as usually used in engineering practice, such a mechanism is inconsistent with the presence of shear forces and varying bending moments. The introduction of additional pure shearing parameters for the beam axis $\bar{v}$, $\bar{w}$ (Fig. 9b) to allow for shear forces, as suggested in (22), does not change the state of affairs and, hence, only discontinuous mechanisms are promising.

Application in Design and Conclusion

The space truss model represents a rational basis for the ultimate strength design of reinforced concrete beams in torsion and bending. Additional design rules are necessary to prevent premature concrete failure, local failure and excessive crack formation under working load. Corresponding design specifications have already been accepted in the Swiss Code SIA-162 RL 34 and in the Model Code of CEB (Comité Européen du Béton), and they are treated elsewhere at length [3, 4]. Taking advantage of the possible plastic redistributions of forces in the longitudinal and stirrup reinforcement, they allow a more economic design of the reinforcement. Moreover the design for shear, torsion and warping torsion can be put on a consistent basis.

The present paper is a contribution to the theoretical background of these developments. A rigorous kinematic or upper bound approach corresponding to the truss model has been missing so far. Allowing easy visualization of the failure model, the new design specifications are based on, the presented basic mechanism may also be helpful to design engineers. Moreover the paper shows that the term "truss model" has rather historical and phenomenological significance. From a theoretical point of view, the model is a strict application of the Theory of Perfectly Plastic Solids to thin-walled beams in torsion and bending governed by the yield condition (5).

Acknowledgement

The study is based on results obtained in the course of a research project on the application of the theory of plasticity to the general plane stress problem of reinforced concrete shear walls under the direction of Professor B. Thürlimann.

Notation

Forces, Stresses

D_s, D_u	resultant of concrete stresses in side resp. bottom shear wall.
L_a	rate of external work.
L_d	rate of energy dissipation.
M	moment.
N_x, N_y, N_{xy}	membrane forces in shear wall, measured per unit length.
n_x, n_y, n_{xy}	membrane forces in concrete, measured per unit length.
P_x, P_y	yield force of x- resp. y-reinforcement, measured per unit length.
P_s, P_u	yield force in side resp. bottom stirrups, measured per unit length.
S	shear flow.
T	torque.
T_v, T_h	torque applied to vertical resp. horizontal shear wall.
Z_o, Z_u	force in top resp. bottom longitudinal stringer.
Z_f	yield force in longitudinal stringer.
z_x, z_y	membrane forces in reinforcement, measured per unit length.
Φ	yield function, plastic potential.
σ_e	steel stress.
σ_f	yield stress in steel reinforcement.

Displacements, Rotations, Strains

u, v, w	displacements.
U, V	warping function resp. circumferential elongation.
ε_x, ε_y, γ_{xy}	strains.
ε_{LK}, ε_{BK}	strains in longitudinal resp. stirrup reinforcement of shear wall K.
γ_K	shear strain in shear wall K
φ	skew rotation.
λ	proportionality factor.
ϑ	angle of twist.

Lengths, Areas, Angles

b	width of cross section.
d	layer depth, distance.
h	height of cross section.
F_x, F_y	area of one reinforcement bar in x- resp. y-direction.
F_0	area enclosed by reinforcement cage.
l, L	length.
r	distance to the shear wall plane from x-axis.
s	circumferential coordinate.
t_x, t_y	spacing of x- resp. y-reinforcement.
x, y, z	coordinate system.
α	inclination of concrete compressive trajectories and collapse cracks; direction of minor principle strain.
β	inclination of discontinuity line or axis of rotation.
δ	angle between y-axis and outward normal to the shear wall.

Subscripts

e	steel.
f	yield.
h	behind, horizontal.
n	normal.
o	top.
s	side.
t	tangential.
u	bottom.
v	front, vertical.
x, y, z	related to x-, y-, z-axis.
I, II	related to major resp. minor principle axis.
L	related to longitudinal reinforcement.
B	related to stirrup.
K	related to the shear wall K.

References

1. Prager, William: Probleme der Plastizitätstheorie. Birkhäuser Verlag Basel und Stuttgart, 1955.
2. Lampert, P.: Bruchwiderstand von Stahlbetonbalken unter Torsion und Biegung. Bericht Nr. 26, Jan. 1970, Institut für Baustatik, ETH Zürich (Dissertation Prom. Nr. 4445, 1970, ETH Zürich), Vergriffen.
3. Lampert, P., Thürlimann, B.: Ultimate Strength and Design of Reinforced Concrete Beams in Torsion and Bending. Sonderdruck aus Band 31/I der Abhandlungen der Internat. Vereinigung für Brücken- und Hochbau, Zürich, 1971, Bericht Nr. 42, Institut für Baustatik ETHZ, Birkhäuser Verlag Basel und Stuttgart, Jan. 1972.

4. THÜRLIMANN, B., GROB, J., LÜCHINGER, P.: Torsion, Biegung und Schub in Stahlbetonträgern. Vorlesungen anlässlich des Fortbildungskurses für Bauingenieure, 9.-12. April 1975, Institut für Baustatik und Konstruktion, ETH Zürich, 1975.
5. MÜLLER, P.: Plastische Berechnung von Stahlbetonscheiben. Bericht in Vorbereitung, Institut für Baustatik und Konstruktion, ETH Zürich.
6. LAMPERT, P., THÜRLIMANN, B.: Torsionsversuche an Stahlbetonbalken. Bericht Nr. 6506-2, Juni 1968, Institut für Baustatik, ETH Zürich, Birkhäuser Verlag Basel und Stuttgart.
7. LAMPERT, P., THÜRLIMANN, B.: Torsions-Biege-Versuche an Stahlbetonbalken. Bericht Nr. 6506-3, Januar 1969, Institut für Baustatik, ETH Zürich, Birkhäuser Verlag Basel und Stuttgart.
8. LAMPERT, P., LÜCHINGER, P., THÜRLIMANN, B.: Torsionsversuche an Stahl- und Spannbetonbalken. Bericht Nr. 6506-4, Februar 1971, Institut für Baustatik, ETH Zürich, Vergriffen.
9. BAUMANN, Th.: Tragwirkung orthogonaler Bewehrungsnetze beliebiger Richtung in Flächentragwerken aus Stahlbeton. Heft 217, Deutscher Ausschuss für Stahlbeton, 1972.
10. NIELSEN, M.P.: Yield Conditions for Reinforced Concrete Shells in the Membrane State, Reprint from Non-Classical Shell Problems, Proc. IASS Symposium, Warswa, Sept. 2.-5., 1963.
11. BRAESTRUP, M.W.: Plastic Analysis of Shear in Reinforced Concrete. Magazine of Concrete Research, Vol. 26, No. 89, Dec. 1974.
12. GVOZDEV, A.A., LESSIG, N.N., RULLE, L.K.: Research on Reinforced Concrete Beams Under Combined Bending and Torsion in the Soviet Union. In Torsion of Structural Concrete, Journal American Concrete Institute, April 1968, p. 310; Publication SP-18.
13. ELFGREN, L., KARLSSON, I., and LOSBERG, A.: Nodal Forces in the Analysis of the Ultimate Torsional Moment for Rectangular Beams. Magazine of Concrete Research, Vol. 26, No. 86, March 1974, pp. 21-28.

Summary

To predict the ultimate strength of reinforced concrete beams with thin-walled closed cross section in torsion and bending, the truss model has proved to be a powerful approach. However, all collapse mechanisms known so far turn out to be incompatible with the latter. In particular, it is shown, why mechanisms such as "Skew Bending" supply different load factors than the truss model. The yield criterion for reinforced concrete shear walls, implicitly used in the truss model, is derived. By means of the corresponding flow rules, new mechanisms are developed being compatible with the state of stress assumed in the truss model. The present study is based on the classical theory of plasticity and on the fundamental theorems of limit analysis.

Résumé

Pour le calcul à la rupture des poutres-caisson à parois minces en béton armé soumises à la torsion et à la flexion, le modèle de treillis jouit d'un succès croissant. Cependant, tous les mécanismes de ruine connus à ce jour se montrent incompatibles avec ce modèle. En particulier, des mécanismes tels que le «Skew Bending» fournissent d'autres valeurs de la charge limite que le modèle de treillis. Le critère de plasticité pour les plaques en béton armé, usé implicitement dans le modèle de treillis, est introduit. A l'aide de la loi d'écoulement plastique correspondante, on développe des mécanismes nouveaux compatibles avec l'état de contrainte supposé dans le modèle de treillis. La présente étude est basée sur la théorie de la plasticité et sur les théorèmes fondamentaux de l'analyse limite.

Zusammenfassung

Zur Erfassung des Bruchwiderstandes von Stahlbetonbalken mit dünnwandigem geschlossenem Querschnitt unter Torsion und Biegung hat sich das Fachwerkmodell als sehr geeignet erwiesen. Dagegen zeigt sich, dass bis heute keine mit diesem Modell verträgliche Kollapsmechanismen bekannt sind. Insbesondere wird darauf eingegangen, warum Mechanismen wie «Skew Bending» zu anderen Traglastfaktoren führen als das Fachwerkmodell. Die dem Fachwerkmodell implizit zugrunde liegende Fliessbedingung für Stahlbetonscheiben wird hergeleitet. Unter Verwendung des zugehörigen Fliessgesetzes werden neue Mechanismen entwickelt, die mit dem im Fachwerkmodell angenommenen Spannungszustand verträglich sind. Grundlage der vorliegenden Arbeit sind die klassische Plastizitätstheorie und die Grenzwertsätze des Traglastverfahrens.

Leere Seite
Blank page
Page vide